Mirror alignment recovery system (MARS) on the Hobby-Eberly Telescope

Wolf, Marsha, Palunas, Povilas, Booth, John, Ward, Michael, Wirth, Allan, et al.

Marsha J. Wolf, Povilas Palunas, John A. Booth, Michael H. Ward, Allan Wirth, Gordon L. Wesley, Darragh O'Donoghue, Lawrence W. Ramsey, "Mirror alignment recovery system (MARS) on the Hobby-Eberly Telescope," Proc. SPIE 4837, Large Ground-based Telescopes, (4 February 2003); doi: 10.1117/12.458034

SPIE.

Event: Astronomical Telescopes and Instrumentation, 2002, Waikoloa, Hawai'i, United States

Mirror Alignment Recovery System (MARS) on the Hobby-Eberly Telescope

Marsha J. Wolf,[*a] Povilas Palunas,[a,b] John A. Booth,[a,b] Michael H. Ward,[b] Allan Wirth,[c] Gordon L. Wesley,[a,b] Darragh O'Donoghue,[d] Lawrence W. Ramsey[e]

[a]University of Texas at Austin, [b]McDonald Observatory, [c]Adaptive Optics Associates, Inc., [d]South African Astronomical Observatory, [e]Pennsylvania State University

ABSTRACT

The Mirror Alignment Recovery System (MARS) is a Shack-Hartmann based sensor at the center of curvature (CoC) of the Hobby-Eberly Telescope (HET) spherical primary mirror used to align the 91 mirror segments. The instrument resides in a CoC tower next to the HET dome, a location which provides a challenging set of problems including wind shake and seeing from two different domes. The system utilizes an internal light source to illuminate the HET and a reference mirror to provide focused spot locations from a spherical surface. A custom lenslet array is sized to the HET pupil image, matching a single hexagonal lenslet to each mirror segment. Centroids of the HET mirror segment spots are compared to the reference spot locations to measure tip/tilt misalignments of each segment. A MARS proof-of-concept (POC) instrument, tested on the telescope in 2001, utilized a commercial wavefront sensor from Adaptive Optics Associates. The final system uses the same concept, but is customized for optimal performance on the HET.

MARS replaces previous burst-antiburst alignment techniques and provides a more intuitive method of aligning the primary mirror for telescope operators. The POC instrument has improved median HET stack sizes by 0.3″ EE50, measured at the CoC tower. The current alignment accuracy is 0.14″ rms (0.28″ rms on the sky), resolution is 0.014″, measurement precision is 0.027″ rms, and segment capture range is ± 5″. With continuing improvements in HET dome ventilation and the addition of software customized for removal of tower motion during measurement, the alignment accuracy is expected to reach approximately 0.04″ rms in the final MARS, to be installed in late 2002.

Keywords: alignment, segmented, primary mirror, Shack-Hartmann, HET, Hobby-Eberly, MARS

1. BACKGROUND

The HET[†] is a 9-meter fixed elevation telescope with a segmented primary mirror. Its Arecibo-style design was a prototypical approach to the construction of a low cost 8-meter class telescope. The telescope structure sits stationary during a science observation, while a tracker at the top follows objects across the spherical primary mirror for up to 2.5 hours at a time, depending on the declination of the object. The constant 35° zenith angle of the telescope maintains a constant gravity vector on the primary mirror and eases its alignment maintenance. The primary mirror is 11 meters point-to-point with a spherical aberration corrector at prime focus that limits the tracking pupil to 9.2 meters. There are 91 hexagonal segments populating the primary, each 1 meter in diameter and supported on a steel mirror truss.

The design specification for HET delivered image quality was 0.6″ 50% encircled energy (EE50), of which 0.56″ was the error budget for the primary mirror. The primary mirror budget allowed for errors in the steel truss, the segment mounts on the truss, segment figure, and segment alignment. The segment alignment portion of the error budget was 0.065″ EE50 for tip/tilt and 25 microns for piston. To meet these requirements, the segments do not need to be phased, but are aligned and maintained for hours at a time. An HET optical design study[1] found that segment tip/tilt errors with a 0.06″ rms distribution cause 0.161″ EE50 of image degradation, and piston errors with a 25 micron rms distribution cause 0.057″ of degradation, the two of which add in quadrature. Segment piston holds fairly well over long periods of

[*] mwolf@astro.as.utexas.edu; phone 1-512-471-0445; fax 1-512-471-6016; University of Texas at Austin, Astronomy Dept., 2511 Speedway, RLM 15.308, C1400, Austin, TX 78712

[†] The HET was funded and built by a consortium of five universities: the University of Texas at Austin, the Pennsylvania State University, the Ludwig-Maxmilians Universität München, the Georg-August-Universität Göttingen, and Stanford University.

Large Ground-based Telescopes, Jacobus M. Oschmann, Larry M. Stepp, Editors, Proceedings of SPIE Vol. 4837 (2003) © 2003 SPIE · 0277-786X/03/$15.00

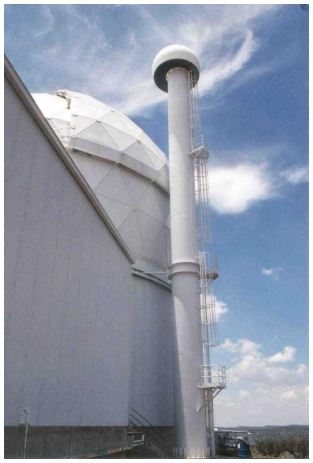

Figure 1: Center of curvature alignment sensor (CCAS) tower.

time, and given its much smaller contribution to image quality errors, the tip/tilt alignment, which changes rapidly with temperature, becomes much more critical to control. Segment piston in the array is set manually with a hand-held spherometer once every few months. This gets the array aligned to an rms piston error of 25 μm, which holds to an average of 70 μm (maximum of 200 μm) over this period of time, which is adequate. Nevertheless, the addition of an automatic piston adjustment technique is planned for the future to eliminate the need of the labor intensive manual procedure and to allow more frequent alignment, especially as the overall image quality of the telescope improves and piston errors begin to have more impact. The alignment techniques described in the remainder of this paper are only for tip/tilt adjustment of the segments.

A tower was built next to the HET dome, shown in Figure 1, to allow placement of an alignment sensor at the center of curvature of the primary mirror. This tower consists of separate inner and outer steel shells to protect the instrument platform on the inner tower from movement due to wind loading on the outside. The radius of curvature of the HET primary mirror is 26.2 meters, requiring the tower height to be about 90 feet. Guy wires stabilize the outer tower, but some motion does get translated to the instrument platform from a common base. This effect places some limits on wind conditions in which the HET mirror can be aligned (40-45 mph) and calls for creative data collection and analysis to remove the effects of tower motion on segment alignment measurements from the tower.

An HET Completion Project[2] was begun in 2001 to tackle known issues that were limiting telescope performance, but could not have been addressed with prior funding. The MARS was part of this effort, along with the Segment Alignment Maintenance System (SAMS)[3,4] and the Dome Ventilation System (DVS).[5]

2. PREVIOUS MIRROR ALIGNMENT TECHNIQUES

2.1. Burst-antiburst stacking

An interferometer for aligning the primary mirror segments, described in Section 2.2, was installed during the telescope construction project, however, a rougher alignment technique was required for initial telescope commissioning. To this end, a technique called burst-antiburst stacking was developed by the onsite staff. The laser projector on the interferometer was used to illuminate the primary mirror from its CoC, and return spots from each mirror segment were viewed on a faceplate back at the instrument in the tower. Because the return spots from an unaligned mirror appeared as an ambiguous bundle of spots on the faceplate, procedures to identify which spots were associated with which segments were required. The mirrors in half the array of 91 segments were tilted such that their spots moved to the edge of the plate, while the other half were aligned. The active half of mirrors were moved such that their spots formed into a ring pattern, or "burst" out from the center into concentric rings. A 3-ring burst pattern on the faceplate is shown in Figure 2. Software automatically went through and searched for spots within a given radius around the locations where they should lie. The code identified spots with specific mirrors, allowing the operator to intervene if things did not look right. A manual mode where the operator selected spots by hand was also available for severely misaligned cases. Once the mirror spots were identified with segments and their positions recorded, the mirrors were sent to the opposite sides of the rings, or "anti-burst." The spots were reidentified and positions recorded. The mirrors were then moved so that each spot was sent to the center. After the first half was done, the procedure was repeated for the other half. The spots were all stacked on top of each other, so the alignment process was called "stacking" the mirror.

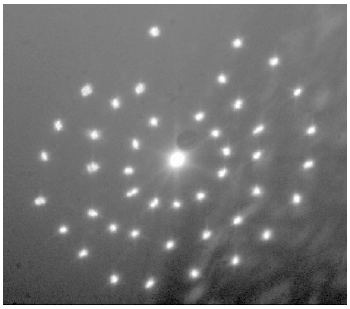

Figure 2: 3-ring burst stacking pattern on the faceplate.

The mirror segment actuators have some hysteresis in their motion, especially in the large (up to 30″) movements required during this method of stacking. The hysteresis varied with seasonal temperature and time, so it was remeasured for each actuator periodically throughout the year. Hysteresis corrections were added into the requested mirror motions

during stacking.

The burst stacking technique was routinely used as the tip/tilt mirror alignment procedure until October 2001, when MARS was installed. It typically produced stack sizes of 1.2″ EE50 at the CoC tower, and on-sky image quality of 2.3″ EE50.

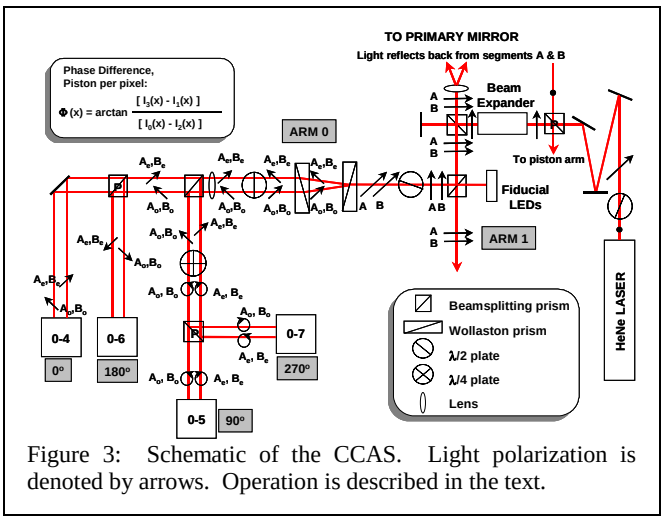

Figure 3: Schematic of the CCAS. Light polarization is denoted by arrows. Operation is described in the text.

2.2. Center of curvature alignment sensor

The Center of Curvature Alignment Sensor (CCAS)[6] was developed by W.J. Schafer Associates, Inc. for alignment of the HET primary mirror. It was intended to align the mirror segments both in tip/tilt and in piston. The sensor was delivered early in the telescope construction project, before the primary mirror was populated with segments. Because of this timing, it was never fully tested on the telescope before the company's branch office that developed the sensor was disbanded. An effort was made by onsite staff in 1999-2000 to debug and test the CCAS in order to make a decision on whether it would suffice as the mirror alignment instrument for the telescope. With a number of bugs corrected, the CCAS did work for tip/tilt mirror alignment under superb environmental conditions, but did not have the robustness required for typical seeing conditions before the DVS, or sufficient capture range for the primary mirror before the SAMS. For these reasons, the CCAS was replaced with MARS during the HET Completion Project. A brief description of the CCAS is given here. More details can be found elsewhere in these proceedings.[6]

The CCAS is a dual-arm polarization shearing Twyman-Green interferometer, schematically shown in Figure 3, that resides at the CoC of the primary mirror. An expanding beam of linearly polarized light from a HeNe laser in the CCAS tower is projected down to fill the HET primary mirror, and reflected back by each segment to a focus at the faceplate. The bundle of return spots, the same spots that were used for burst-antiburst stacking, is sent through a pinhole in the center of the faceplate and into the instrument. This cone of light is collimated, split, and sent into both the tip/tilt and piston measurement sections of the instrument. Only the tip/tilt measurement is described here, since that was the only part of the instrument used on the HET. Details on its piston measurement technique can be found in the CCAS paper in these proceedings.[6]

The collimated beam is split into 2 arms, denoted as Arm 0 and Arm 1 in Figure 3. Only Arm 0 is shown in the figure for clarity, since the two arms are identical except for image shear direction. Light polarization orientation is indicated in the figure by arrows. The beams in each of these arms go through a pair of Wollaston prisms, which shear the image of the HET primary. The Wollaston prism angularly separates the image into two that have polarizations 90° out of phase, the ordinary and extraordinary rays (denoted as o and e in Figure 3). The second Wollaston prism in the pair is reversed with respect to the first and undoes the angular deviation of the beams, sending them out parallel and separated by a distance that overlaps a mirror segment in one image with its neighbor in the other image. An interference pattern is created on every segment in the overlapped image of the primary. Such an interferogram of half of the primary mirror array is shown in Figure 4. If two segments were perfectly aligned, you would see only 1 fringe on the segment. As tips and tilts are introduced between the two mirror segments, more horizontal and vertical fringes appear. The second arm of the instrument does exactly the same thing, except that the shearing direction is 120° from the first, causing every segment in the array to be overlapped with a neighbor in at least one of the arms. The shear direction in Figure 4 is indicated by the arrow. The columns of segments on the left and right sides have no fringes because their images did not overlap a second segment image.

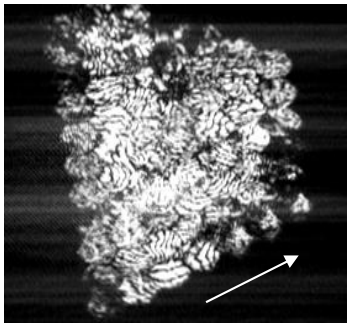

Figure 4: CCAS interferogram of segment tip/tilts for half the HET primary mirror array. The arrow indicates the image shear direction. Dome seeing effects blur out the fringes in some locations.

The boxes labeled 0-4, 0-5, 0-6, and 0-7 in Figure 3 represent cameras in Arm 0. Optics leading up to each camera introduce known phase shifts of 0°, 90°, 180°, and 270° into each split off beam. By comparing the fringe patterns in each of these 4

images, the phases due to tip/tilt misalignments of the 2 segments are calculated. Corrections required for these tip and tilt misalignments are sent to a mirror correction file that is applied to the mirror segment actuators to align them.

The CCAS saw very limited use on HET. The instrument's capture range of 0.36″ was too small to be of use for initial mirror alignment, especially before the SAMS was installed. In principle, the CCAS could have been used to fine tune the tip/tilt segment alignment after a burst-antiburst stack, if the dome seeing conditions were excellent and the fringes were clear, but in practice, this very rarely happened over the entire mirror array. However, the CCAS could be used to improve alignment on smaller groups of mirrors, up to 23 segments. It was successfully used for initial verification testing of the SAMS on a group of 7 mirror segments. The instrument concept worked, just not through 52 meters of uncontrolled atmosphere over an 11 meter aperture in this application.

3. MIRROR ALIGNMENT RECOVERY SYSTEM (MARS)

In May 2001, the decision was made to find a more robust and precise method for aligning the HET primary mirror. Because of its widespread and successful use in similar applications, the Shack-Hartmann wavefront sensor was at the top of the list for this task. A proof-of-concept instrument was devised to test the Shack-Hartmann technique on HET. This system, the Mirror Alignment Recovery System Proof-of-Concept, or MARS-POC, was installed in September 2001. In spite of its "proof-of-concept" state, it was superior to previous methods and has subsequently been used as the mirror alignment instrument for HET. Things learned from the POC instrument have been incorporated into the design of a final MARS, which will be installed in late 2002.

3.1. Shack-Hartmann proof-of-concept instrument

MARS is built around a commercial Shack-Hartmann wavefront sensor. A schematic of the POC instrument is shown in Figure 5. Figure 6 is a photo of the front end optics. An expanding white light beam, with its source originating through a fiber-fed pinhole at the CoC of the HET primary mirror, is projected down to fill the primary. Each mirror segment in the HET array reflects a portion of this light back, all beams coming to a focus again at the CoC on the back side of the beamsplitter cube. A collimator lens is placed its front focal length away from the CoC. This lens actually serves two purposes. One is to collimate the HET return beam, the other is to image the primary mirror array. The next optical component is a lenslet array which is placed at the image plane of the HET primary mirror. The custom lenslet array is sized such that each hexagonal lens falls on top of a mirror segment in the image of the primary mirror, shown in Figure 7. The lenslet array mounts to the front surface of the WaveScope, a commercial wavefront sensor manufactured by Adaptive Optics Associates (AOA) and used as our POC Shack-Hartmann sensor. Inside the WaveScope is a CCD camera on a translating stage. The moving stage allows the CCD camera to image either the focused spots from the lenslets, or the lenslet array itself, which is coplanar with a pupil image of HET primary mirror.

A knife edge at the back face of the beamsplitter cube allows the entire instrument to be placed at the correct focus before a measurement is made. Knife edge focusing, while watching a real time HET pupil image on the MARS camera, places the back face of the cube at the HET CoC.

An internal reference beam can be sent into the WaveScope for calibration. This beam consists of light reflected from a reference sphere that has its CoC at the same point in space as the HET's, at the back face of the beamsplitter cube. The lenslet array samples light from the reference mirror and each lens focuses spots whose locations correspond to those from a "perfect" sphere, analogous to a perfectly aligned segmented mirror. The positions of the HET spots on the CCD are compared to the positions of the reference spots. Differences in these positions, caused by misaligned mirror

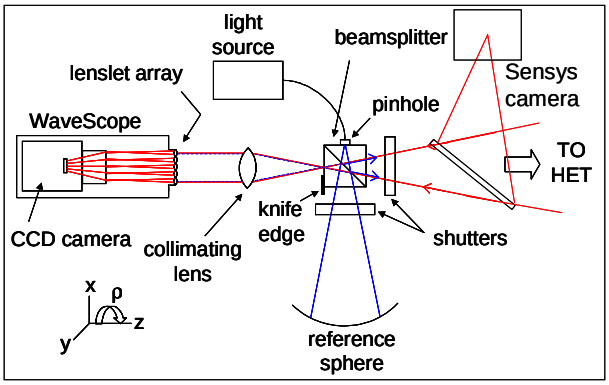

Figure 5: MARS-POC schematic, top view. Light expands from a fiber-fed pinhole on the side (top here) of the beamsplitter cube, reflects down to and illuminates the HET primary, returns to focus at the primary's center of curvature on the back (left here) side of the cube, is collimated by a lens, encounters the lenslet array which has each lens matched to an HET segment, then is focused and imaged onto a CCD camera. Another leg contains a spherical reference mirror for calibration, shown at the bottom of this schematic. The thin beamsplitter to the right provides an image of the entire mirror stack returned from the HET to the Sensys camera.

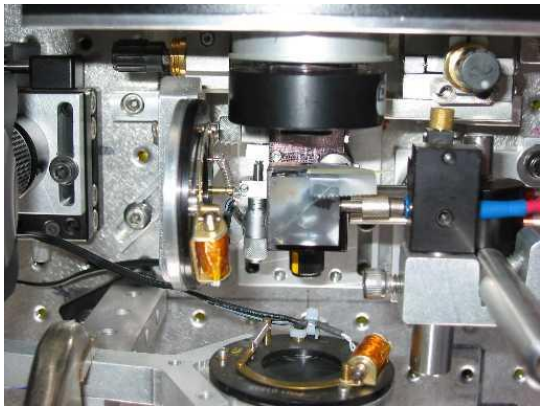

Figure 6: MARS-POC optics. In this photo, the WaveScope is up and the HET is down. The lenslet array mount is the silver cylinder near the top, the black cylinder below that is the mount for the collimator lens, the glass square in the center is the beamsplitter cube, the Center of Curvature is at the back face (top in photo) of the cube, a temporary knife edge is affixed to the back of the cube, the fiber-fed light source is just to the right of the cube, a pinhole is glued to that side of the cube, the reference beam shutter is to the left of the cube, the reference mirror is further to the left and just off the edge of the picture, the HET shutter is at the bottom of the picture. For scale, the beamsplitter cube is 1 inch on a side.

segments, measure tips and tilts of each segment. Corrections are then sent to the mirror positioning system to align the HET primary.

A pellicle beamsplitter is placed in front of MARS to send a small percentage of the HET return beam to a Sensys CCD camera for imaging the whole stack. This camera is where stack sizes are measured.

3.1.1. Optics

3.1.1.1. Design

MARS optics were selected such that the 1-meter diameter HET segments were scaled down by approximately 1000:1 to a 1-mm image size. This also meant that the pitch of the matched lenslet array would be approximately 1 mm. Given the HET's 26-meter radius of curvature, the collimator lens needed to have a focal length of about 26 mm for this demagnification. With this amount of reduction tilt angles of the segments are magnified by a factor of 1000, so 5″ becomes 5000″, or 25 mrad, at the lenslet array. The standard WaveScope CCD relay lens provides a demagnification of 0.42 to the CCD's 10 micron pixels, resulting in an effective pixel size at the lenslet focal plane of 24 microns. To keep a mirror spot under its 1 mm diameter lenslet, the maximum spot displacement should be about ± 400 microns. Given a maximum segment tilt of 25 mrad, this says that the lenslet focal length should be 16 mm. For this focal length, a pixel subtends 1.5 mrad at the lens array, or 1.5 μrad (0.3″) at the primary. Assuming that we can centroid to 1/10 pixel, this should give a resolution of 0.015″ (extra factor of 2 because with mirrors angular movements are doubled).

For good centroiding, spots on the CCD camera must be well sampled. The spot size on the CCD is set by seeing when measuring the HET primary and will always be larger than 1 pixel. However, the reference mirror spots from a point source with no local seeing would be too small, as the diffraction limited spot size from the f/16 lenslets is only about 16 microns null-to-null at 500 nm. Therefore, we chose to use a resolved reference source. This could be achieved by using a pinhole on the light source with a size of 130 microns, resulting in spots that are approximately 3 pixels across at the CCD.

The aperture of the collimator needed to be large enough to not vignette the pupil image of the 11 m primary mirror, requiring at least an 11 mm lens aperture for the 1000:1 reduction. To this must be added about 1.5 mm to allow for spot displacements at extreme segment tilts. This required the f/# of the collimator lens to be ≤ 2.1.

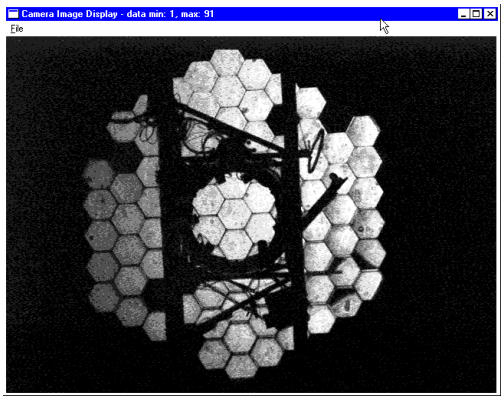

Figure 7: HET pupil image from MARS. Each lenslet falls on top of an HET segment. The shadow across the mirror array is from the tracker (without the Prime Focus Instrument Package installed). Black segments are either missing from the mirror array, or misaligned beyond the capture range of MARS. The few partially illuminated segments are just at the edge of capture range.

3.1.1.2. Actual System

Off the shelf standard optical components were used where ever possible to get the proof-of-concept instrument together quickly and test the technique. For this reason, the actual optics used vary slightly from the design, but do not significantly change the resulting numbers. The collimator lens is an f/1.6 with a focal length of 25 mm, instead of 26 mm This makes the demagnification slightly

higher, 1046:1 rather than 1006:1, so the size of the HET segment image is a bit smaller than 1 mm. The image of the HET was measured with our collimator lens at its proper location in the tower and the lenslet array was manufactured to exactly match the segment image size. The focal length of the lenslets in the array came out as 17.6 mm, instead of 16 mm. This means that the segment spot displacement on its lenslet for a 25 mrad tilt becomes 447 μm instead of 400 μm, possibly causing more confusion between neighboring spots since it travels closer to the boundaries between subapertures. The actual lenslet focal length results in a slightly better estimated resolution of 0.014″, assuming 1/10 pixel centroiding. A 100 μm pinhole, rather than 130 μm, was used on the light source, which is the correct size to give a spot size on the CCD of approximately 3 pixels for these optics. We also added a V filter to the white light source to cut down chromatic aberration from the fast collimator lens. The spherical reference mirror is an f/1 with a 2-in diameter and 2-in focal length.

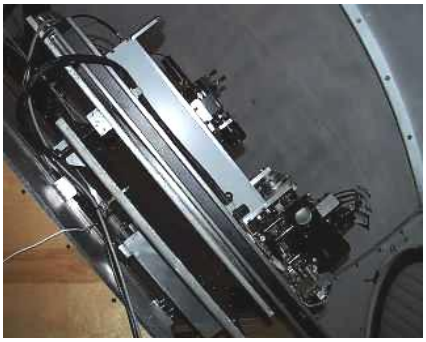

Figure 8: The MARS-POC on its wedge mount in the CoC tower. The circular shutter in the lower right corner of the picture opens, allowing access to the HET when it is pointed at the tower.

3.1.2. Mechanical layout

The MARS-POC resides in the CoC tower, 26 meters from the primary mirror. The instrument is mounted on a wedge that places it on the optical axis of the HET, which sits at a fixed elevation of 55°. Figure 8 shows MARS on its wedge in the tower. Because the 90 ft tall tower shrinks, grows, and bends with temperature, the instrument must be moved around to find the true CoC before each use. Translation slides provide remotely controlled x-y (horizontal-vertical) translation and focus (to/from HET) motions for the entire optical bench. The actuators used for these motions are from TS Products, the same as those used for positioning HET mirror segments. To offset the weight of the optical table for the focus motor, a customized counterweight hangs off the back side of the wedge. Manual angular adjustments on the table allow initial alignment to the HET in pitch and yaw.

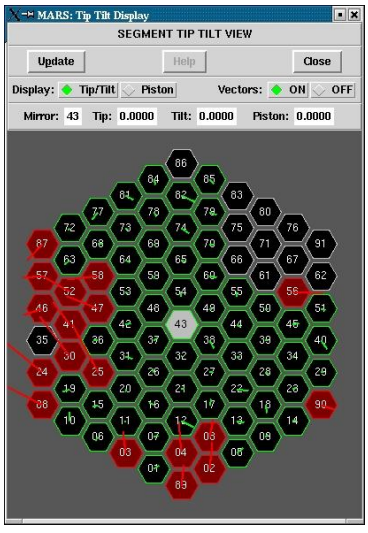

Figure 9: Segment tip/tilt error display on the MARS operator console. Vectors on each segment show the direction and magnitude of measured alignment errors. Segments outlined in green have measured errors within spec (0.06″), red are out of spec, and gray are not measurable or are obscured by the tracker.

3.1.3. Control system

To interface the WaveScope, an off the shelf product, to the current HET control system four major components were addressed: 1) passing of tip/tilt corrections to the primary mirror control (PMC) system, 2) control of light path shutters, 3) visually displaying the tip/tilt corrections for the telescope operators, and 4) remote translation of the MARS platform to allow telescope operators to align and focus the WaveScope to the HET. The interface was accomplished by the creation of a set of intermediary programs that would act as a server/controller for the entire MARS system. This set of tightly interlaced programs is collectively known as the MARS software, written in Tcl/Tk and C.

The WaveScope software was modified to allow shutter open and close commands, sent via a TCP/IP socket to the MARS software server. Command is then passed to the hardware control section of the MARS software for implementation. The tip/tilt corrections are collected by the MARS software, which serves a PMC TCP/IP client interface allowing the PMC to request new tip/tilt corrections for each mirror segment. The system also archives all tip/tilt corrections generated by the WaveScope software.

The MARS software runs a graphical user interface (MARS GUI) which allows the HET telescope operators to control the motors that move the MARS platform. It gives the telescope operators manual control of the beam shutters, as well as power supply control for each component of the MARS/WaveScope hardware, and displays measured segment tip/tilt errors to the operator (Figure 9).

All computers for the MARS-POC are located in the HET control room. RS-232 communication, Ethernet, and video links to the CoC tower are achieved via fiber

optic cables for lightning isolation.

3.1.4. Alignment

3.1.4.1. Normal operation

Because the MARS sits atop a 90 ft steel tower that changes in height with ambient temperature, bends from solar heating on various sides during the day, and cools off during the night, the instrument is never in exactly the same spot relative to the HET when the telescope operator needs to stack the mirror. Using views from the internal MARS camera, the operator translates the entire wedge in x and y to center up the HET return beam. A knife edge focus is performed to adjust the distance of MARS from the HET. This is accomplished by translating MARS sideways such that a fixed knife on the back of the beamsplitter cube cuts into the HET return and adjusting the focus until the MARS light source pinhole and return beam focus are coincident at the primary mirror CoC. These adjustments of 3 axes to position MARS are all the alignment required in normal operation. No angular adjustments of MARS are routinely required to align to the telescope, since the elevation of the HET is fixed and its azimuthal positioning is good to 0.003^{o} for pointing at the CoC tower.

3.1.4.2. Initial setup

A more rigorous and manual procedure must be followed to initially align the internal optics of MARS. The optical axis of the instrument is set by the motion of the translation slide of the WaveScope CCD camera. When this translation axis is aligned to the optical axis of the HET, no motion of the HET return beam on the CCD camera occurs as the stage moves. Alignment begins with the WaveScope in its nominal location and the pellicle beamsplitter out front. (Refer to Figure 5.) A laser beam is reflected off the back side of the pellicle and into the WaveScope. The beam is aligned such that no spot motion occurs on the CCD when the stage is translated. MARS optics are then placed into position at their nominal distances on the optical table, centered with the laser beam, and made normal to the optical axis using their laser back-reflections. We begin with the beamsplitter cube, then the reference mirror such that its return falls onto the back side of the pinhole light source on the beamsplitter cube, then the collimator lens, and finally the lenslet array. After the optics are in place, the white light source through the pinhole is used for fine tuning of the centering and perpendicularity of each component to the optical axis of the instrument. The distance of the reference mirror is adjusted by performing a knife edge focus at the back face of the beamsplitter cube, placing the reference mirror CoC at this back face.

The spacing of the collimator lens from the beamsplitter cube and its tilt relative to the optical axis are set by using the WaveScope itself to measure tilt and focus errors between the reference beam focused spots and the lenslet centers on the CCD. The precise placement of the collimator lens is adjusted to minimize these errors.

The remaining steps use the white light returned from the HET and require a couple iterations. After x-y centering of the whole MARS wedge, the pitch and yaw angles of the optical table on top of the wedge are adjusted to place the instrument on the optical axis of the HET. This can be accomplished by running the CCD translation stage back and forth and watching for image motion on the CCD as it goes from a pupil image of segments to focused spots. Next, the distances of MARS optics are fine tuned. The back face of the beamsplitter cube is placed at the HET CoC by performing a knife edge focus there and moving the focus of the entire table. Then comes the distance from the collimator lens to the lenslet array. The lenslet array must be placed at the back imaging plane of the lens, such that a crisp image of the HET primary falls at the plane of the lenslet array. Because the lenslet array attaches to the front of the WaveScope, this adjustment is accomplished by translating the entire WaveScope along the optical axis with adjusting screws. The CCD camera is placed at the stage location for viewing the pupil image. The lenslet array is removed, and the WaveScope body is translated along the optical axis until the HET primary image is in focus on the CCD. The lenslet array is replaced and adjusted in x (horizontal), y (vertical), and rotation until the hexagonal lenses line up perfectly with the HET mirror segments.

Since the WaveScope was moved in previous steps, a second iteration of fine tuning the collimator position and tilt is done using the WaveScope tilt and focus error measurements for the reference beam. The HET return beam is then sent into the instrument, with the reference beam blocked, the entire MARS is translated in x and y to center up to HET, a knife edge focus is done to place MARS at the HET CoC, and then the pitch and yaw angles on the optical table are readjusted to fine tune the alignment of MARS to the HET.

3.1.5. Software and data analysis

The software suite that supports the WaveScope Hartmann wavefront sensor consists of an extensive library of data manipulation and display routines written in the C programming language that are assembled into various functional sequences under the Tcl scripting language. The use of this interpreted scripting language as the top level of the software allows rapid development of new sensing procedures. The software developed for this segment alignment sensor application represents just such a case. No new lower-level algorithms were needed for this effort. The existing routines were simply arranged in the proper sequence and supplied the required data to allow calculation of the primary mirror segment tilts.

In normal operation the WaveScope sensor collects a set of seven images that are used for the full calibration and measurement of a wavefront. Four images are obtained using the reference source. These consist of two images of planes on either side of the Hartmann lenslet array, which show bright and dark grids produced by the edges of the lenslets. These grid images are analyzed to determine the locations of the centers of all the lenslets in camera coordinates. A second pair of images is taken at planes slightly inside of and at the lenslet focal plane. These images are used to unambiguously associate each Hartmann spot with the lenslet that generated it by projecting the chief ray in each subaperture back to the lenslet plane. The result of the analysis of these four images is a matched list of reference spot positions and associated lenslet centers.

Three images are then obtained using the test source. One is an in-focus image of the test pupil. This allows the position and size of the pupil to be determined in camera coordinates. This information can be combined with the coordinates of the lenslet centers to determine the location of each Hartmann subaperture within the test pupil. Again, two images are obtained just inside of and at the lenslet focal plane. These images are used for two purposes. The in focus image is analyzed to locate all spots that meet certain criteria that assure they are suitable for making a subaperture tilt measurement. Only the spots meeting these criteria are used in the wavefront measurement. The in-focus and inside-focus images are used to associate the selected spots with the lenslets that formed them. This results in a second matched list of test spot locations and associated lenslet centers.

The locations of the lenslet centers do not depend on whether the reference or test source is being observed. Thus the lenslet center locations in each of the matched lists produced by the above procedures are subsets of the same, complete list generated from the pair of reference pupil images. The two lists are matched to each other and a list of lenslet centers in common to both is derived. This list represents the final set of Hartmann subapertures that will be used in the measurement. The locations of the reference and test spots associated with each lenslet in this list are differenced to produce the subaperture tilt estimates.

The modifications to this standard procedure for the MARS are quite straightforward. The same four reference source images are collected and processed in the standard way. Because the relation of the test pupil to the Hartmann lenslet array is fixed by the optical system, no test pupil image is collected, just the two test spot images. Again, these are processed in the standard way to produce the final matched list of test and reference spot positions with their associated lenslet centers.

Because the sensor identifies valid spot images each time a measurement is made, it automatically adapts for the varying obscuration of the primary produced by the HET tracker. For any tracker position, the sensor will report tilt measurements only for those subapertures that receive sufficient light.

The final step in the processing of the tilt data is specific to this application. During the commissioning of the instrument, a table was generated that associated the location of the center of the image of each mirror segment, in camera coordinates, with the identification number of that segment. This list is then used in one further matching process. The final list of matched test and reference data associates each measurement with a lenslet center. Since the lenslet centers are optically matched to segment centers, by matching lenslet centers to the list of segment centers it is possible to connect the segment identification number with the segment tilt measurement for each subaperture.

During a MARS measurement on HET, 25 reference images and 50 HET images are saved. A sampling frequency of 5 Hz over a period of 10 sec is used to mitigate typical seeing events with this timescale. Centroids of all the spots are calculated in each image and the 50 centroids are averaged together for each mirror segment. From the centroids, tips and tilts are calculated, based on differences from reference spot locations. The tip/tilt values of the central mirror segment in the HET array are subtracted off of all segments to remove global errors induced by tower motion during the

measurement. The tips and tilts of each mirror are written to a file and corrections are sent to the primary mirror computer that controls the segment actuators. This process is repeated 2-3 times until tip/tilt errors of all segments are within alignment spec. Once all the mirror segment moves are complete on the final stacking iteration, the SAMS loop is closed to maintain the alignment of the primary mirror.

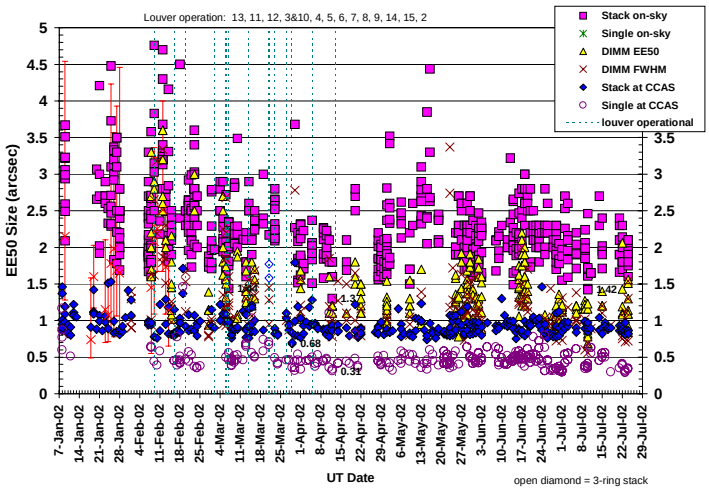

Figure 10: HET stacking and image quality history for Jan-Jul 2002. All values are EE50 sizes except as otherwise noted. Filled diamonds are stack size at the CCAS tower, open circles are single mirror segment size at the CCAS tower, filled squares are on-sky pre-science exposure image size, X's are DIMM FWHM, triangles are DIMM numbers converted to EE50 by a factor of 1.2. Dotted vertical lines indicate when individual louvers were installed for dome ventilation.[5] The error bars on some DIMM points denote the max and min for that night with the median for the night marked by the X. DIMM points without error bars are instantaneous readings throughout a night. The 2 open diamonds were 3-ring burst stacks and fall well above the MARS stack values.

3.1.6. System performance

3.1.6.1. Stack Size

A history of HET stacking and on-sky image quality (IQ) is given in Figure 10 for Jan-Jul 2002. The MARS is stacking to a median size of 0.9″ EE50, measured at the CCAS tower. This compares to 1.2″ EE50 before MARS. The minimum stack size achieved with MARS to date has been 0.68″. On-sky IQ does not reflect improvements in stack quality, as it is dominated by dome and intrinsic site seeing. On-sky IQ for Jan-July 2002 has a median of 2.2″ EE50 (~ 1.8″ FWHM), compared to on-sky IQ of 2.3″ EE50 for the year before MARS was installed. Dome ventilation by louvers and intrinsic site seeing improvements during summer months do seem to have an effect on the upper envelope of on-sky points. Site seeing at the HET has been monitored with differential image motion monitors (DIMMs) over the past year.[7] They give a median site seeing over this period of 1.05″ FWHM at the zenith, 1.19″ at the HET declination, with a standard deviation of 0.29″. In initial comparisons, not much correlation is seen between HET IQ and DIMM measurements, suggesting that we are still limited by dome seeing from heat sources inside the dome. These are being addressed in the continuing HET completion project.[2] As dome seeing improves, we expect that stack sizes will also improve. The following subsections within 3.1.6 discuss stacking errors and present data to support this claim.

3.1.6.2. Accuracy, resolution, and precision

The measurement resolution of the MARS-POC is 0.0143″. Segment alignment accuracy is currently 0.14″ rms (0.28″ on the sky), with a 0.027″ rms measurement precision (1/6 pixel in tip and tilt). A number of factors affect the performance of the instrument, including mirror segment figure, centroiding precision, CoC tower motion, dome seeing, and the global radius of curvature of the primary mirror. Each of these items are addressed in the following subsections.

3.1.6.3. Segment figure

The specifications for HET mirror segments called for an optical figure of 0.052 λ (0.033 μm RMS) over the spherical surface and radii of curvature (RoC) all matched to within 0.5 mm, with a target RoC of 26,165 ± 10 mm (actual master sphere had 26,163.92 mm). The mirrors were tested on HET mounts at a 55° elevation angle at Kodak[8] and met the specifications when delivered, but once placed on their mounts in the HET array some have deformed. Some of these cases are due to broken flexures in the mounts that cause the mirror to bind on its central hub. Some are due to clocking of the segment such that the mount binds, because of improper placement relative to the gravity vector at its position in the array. Problematic segment mounts are being identified and dealt with as part of HET's routine maintenance. The result of these mount problems is that distorted mirror figure causes some of the focused segment spots to be double-lobed, donut-shaped, or astigmatic, all of which can cause centroiding problems and add to measurement noise in MARS. Average segment spot sizes (from a resolved 100 μm pinhole source) were 0.64″ EE50 at the time of this

analysis (0.46″ EE50 now after installation of louvers) with an average ellipticity of 0.14, both depending somewhat on dome seeing at the time the images were taken. Some of the spot quality problems are due to dome seeing, as evidenced by their observed variability.

3.1.6.4. Synthetic stacks

To investigate the significance of segment figure on stacking errors, synthetic stacks were generated using actual single segment spot images. To accomplish this the mirror array was burst out into a hexagonal pattern so that all segments could be seen at once. Postage stamp subsections around each segment spot in the hexburst image were extracted and centroids determined. The individual images were shifted and combined to simulate an overall mirror stack. Aligned perfectly, the spots produced a stack image of 0.64″ EE50, consistent with the average size of a single segment. Stacking errors were added by combining the individual spot images with random offsets derived from a Gaussian distribution and also by using actual measured tip/tilt offsets from MARS. Both alignment offsets produced similar stacks, suggesting that the Gaussian error distribution was valid. Figure 11 shows a plot of synthetic stack size vs. rms stacking error, σ. The filled circles use 91 individual segment spot images and the open circles use 91 images of the best segment. The solid lines are stack sizes calculated from the equation in Figure 11. Note that the segment alignment angular errors are multiplied by a factor of 2 because of the mirror reflection before being applied to the spot images; hence, 2 sigma appears in the equation giving the quadrature sum of alignment error and single segment image size. The factor 2.35 converts sigma to FWHM, 1.2 is an empirically derived relation between FWHM and EE50, and indiv(EE50) is the EE50 value for a single segment image (0.64″ for the average, 0.45″ best). The plotted lines follow the points very well for sigma < 0.075″, but then depart, probably due to the fact that the conversion between FWHM and EE50 was derived from HET images with EE50 > 1.8″, and this factor is known to decrease with smaller images. The plot shows that typical MARS stacks of 0.9″ EE50 have maximum rms stacking errors of 0.14″. It also indicates that stack sizes should improve by 0.05-0.2″ EE50 with better segment spot images.

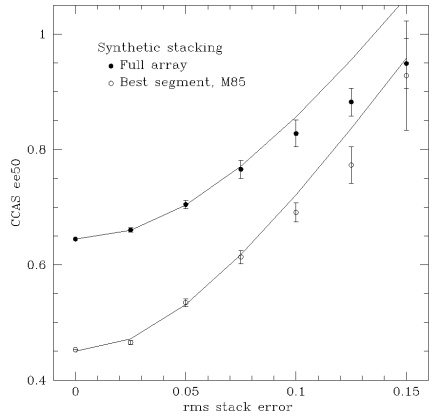

$$stack(EE50) = 1.2\sqrt{[2\sigma(2.35)]^2 + \left(\frac{indiv(EE50)}{1.2}\right)^2}$$

Figure 11: Synthetic stacks using actual single segment spot images. The vertical axis is the stack size measured at the CCAS tower. Solid points use 91 individual spot images, open points use 91 images of the best segment. Solid lines are stack sizes from the equation above. See the text for details. Current MARS stacks of 0.9″ EE50 have maximum rms stacking errors of 0.14″.

3.1.6.5. Tower movement

Tests were conducted to investigate the effects of tower shake from wind loading on MARS measurements. A total of 250 MARS spot images of the HET were collected at a rate of 15 Hz over a 17 sec period. The wind during this test was 17-24 mph from an azimuth of 300° (the CCAS tower sits at 68°). All spots in each image were located and centroided using the *starfind* and *center* routines in *IRAF*.‡ The spot positions over the sequence were matched up to individual segments using the *xyxymatch IRAF* routine, and average positions for each segment were calculated. Measurement noise and global motions associated with the tower were examined by analyzing the movement of spots from their average positions. Tower motion was clearly seen as a global oscillation of all the segment spots with time at a frequency of 1.25 Hz. The rms deviation of the spots after subtracting the tower shake is residual noise in the measurement. The geometric mean of measured tip and tilt tower motions was 0.067″, leaving residual spot motions of 0.041″. The rms amplitude of tower motion varies linearly with wind speed as 0.0029″ mph^{-1}. For wind speeds of 24 mph the predicted rms tower shake is 0.07″. (At wind speeds of about 40-45 mph tower shake becomes too great to stack with MARS.) With proper subtraction of tower movement, tip and tilt errors are measurable to an rms error of 0.04″. Tower motion removal will be fully implemented in the final MARS.

3.1.6.6. Dome seeing

An examination of the tower subtracted motions for individual spots shows that some segments have dramatically more

‡ *IRAF* is distributed by NOAO, which is operated by AURA Inc., under contract to the NSF

residual noise than others. Deviations in the motion for individual segments have time scales of order 5 to 10 seconds. Analysis of these motions as a function of segment location in the primary array shows a strong spatial correlation in the amplitude of the residuals to tracker proximity, suggesting that spot motions are due to localized seeing from heat sources on the tracker. The implied segment misalignment angles from RMS amplitudes of spot motions across the array vary from 0.027″ to 0.1″, depending on distance from the tracker. Spot motions due to seeing events have been tracked across the primary mirror at rates of 1 m sec^{-1} if at the primary and 0.5 m sec^{-1} if at the height of the tracker. The rms motions of "quiet" segments well away from the tracker show a constant value of 0.027″, which may be the centroiding noise floor of MARS. This corresponds to 1/6 of a pixel on the WaveScope CCD camera in tip and tilt.

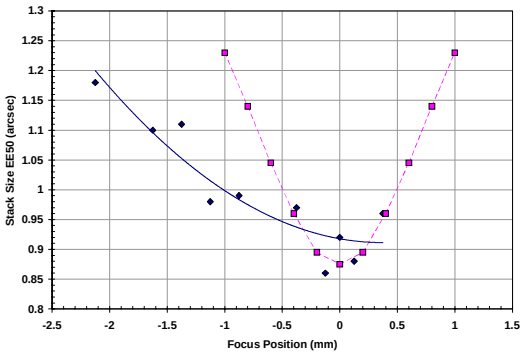

Figure 12: Image quality vs. primary mirror GRoC. Filled diamonds are data from a MARS GRoC stacking test. Each point was the stack size when the primary was aligned at that MARS focus position. The solid line is a 2nd order polynomial fit to the data. Filled squares are points from the SALT optical model with stack sizes scaled up by a constant factor to match that of HET.

3.1.6.7. Global radius of curvature

During a MARS stack the global radius of curvature (GRoC) of the primary mirror is set by a knife edge focus or by minimizing the spot size at the stack camera of a segment with an RoC close to the mean of all segments, R_{seg}. Optical design studies by the SALT team have predicted an image quality degradation of 0.46″ EE50 per mm departure of R_{GRoC} from R_{seg}, where R_{GRoC} is the RoC of the primary mirror.[9,10] Stacking tests with MARS have shown stack degradation due to GRoC error of about 0.28″ mm^{-1}. The spread in RoCs of the HET segments is approximately ± 1 mm, while the spec was ± 0.25 mm. This large spread is likely due to segment distortions from the mount problems mentioned in Section 3.1.6.3. It is expected that the observed stack degradation would approach the design study predictions if the actual spread of segment RoCs was smaller. In any case, stack size improvements of 0.34″ EE50 have been seen by finding the correct GRoC at which to stack during MARS commissioning. Data from such a GRoC stacking test are shown in Figure 12.

3.2. Final MARS design

The final MARS will be conceptually the same as the MARS-POC, but will incorporate some improvements. The opto-mechanical layout of the final MARS design is shown in Figure 13. The commercial WaveScope hardware will be replaced by an optical bench containing a different CCD camera, a translation stage for the camera, an adjustable mount for the customized lenslet array, a collimator lens matched to the new CCD camera, the beamsplitter cube, the reference mirror, and the pinhole light source. Mounts for all components will be sturdier and have more adjustment than those on the POC system.

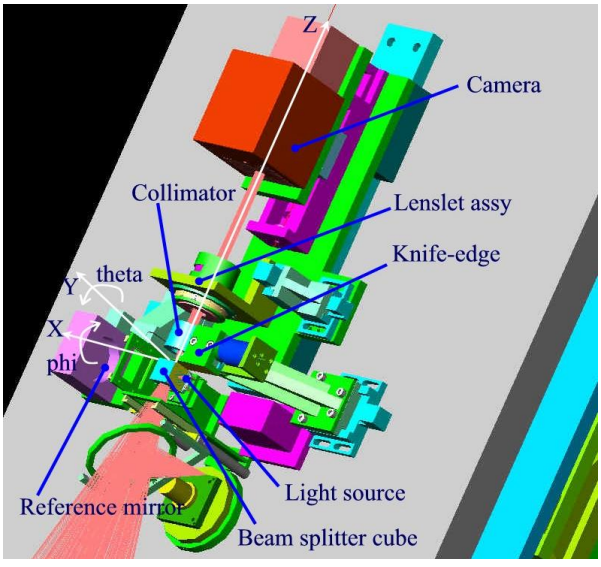

Figure 13: Opto-mechanical layout of the final MARS.

The CCD camera will have a larger chip (1024x1024 vs. current 768x494), more dynamic range (10-bit vs. current 8-bit), digital data or analog progressive scanning interline transfer output (vs. current interlaced transfer RS-170 output into frame grabber card), and a 40 MHz clock speed. These changes will result in better spatial resolution, allowing a larger image size on the chip and thus a longer focal length, higher optical quality collimator lens; better spot detection above the background with the higher dynamic range; and faster data collection for tower motion removal with the 40 MHz clock speed.

About half of the time required to perform a primary mirror

alignment with the MAR-POC is spent in knife edge focusing, to place the instrument at the HET CoC. In the final MARS, the knife edge will be separated from the beamsplitter cube and operated remotely in 2 modes. A fast mode will slide the knife edge into the beam with a pneumatic cylinder, and a slow mode will be controlled by the operator via a voice coil actuator. This should ease and speed up focus position interpretation by placing the motion control directly into the hands of the operator. It will also keep the knife well out of the beam when not in use, so that it will not limit capture range by blocking spots at large tilt angles. Automated image-based focusing is also being investigated for the final MARS.

A Linux version of the AOA WaveScope software will be used for instrument control and analysis. Improvements will be added through specialized routines to sample data at a fast rate and remove tower shake during measurements, and to improve the spot following routines to increase capture range for misaligned segments. Hardware will be controlled through a Programmable Multi Axis Controller (PMAC) II from Delta Tau Systems.

4. SUMMARY

Though installed as a proof-of-concept test of the Shack-Hartmann technique for aligning the HET primary mirror, the MARS-POC very quickly began improving the HET stacks. It has been used as the alignment instrument for the telescope since its installation, and has improved median stack sizes from 1.2″ to 0.9″ EE50. The POC instrument has a segment alignment accuracy of 0.14″ rms, a measurement resolution of 0.0143″, a measurement precision of 0.027″ rms, and a segment capture range of ± 5″. The POC system has been used to identify areas for improvement, which are being incorporated into a final MARS to be installed in late 2002. With these changes in the instrument, and continuing dome seeing improvements, the final MARS is expected to reach an alignment accuracy of 0.04″ rms. At this accuracy, HET image quality will not be limited by the initial alignment of the primary mirror.

ACKNOWLEDGEMENTS

The authors would like to thank Grant Hill, Matthew Shetrone, and John Glaspey for their work on developing the burst-antiburst stacking technique. We acknowledge the team at W.J. Schafer Associates, Inc. who designed and built the CCAS, and thank Victor Krabbendam, Bill Gressler, and François Piché for their initial work on deciphering, debugging, and testing this instrument. We thank Jennifer Roberts for support during the assembly and testing of MARS optics at AOA. We also sincerely thank the entire HET staff, past and present, for many hours of assistance in testing and improving primary mirror alignment on the telescope.

REFERENCES

1. P. MacQueen, “SST Optical Design study,” SST Technical Report #57, July 1991.
2. J. Booth, M. Wolf, J. Fowler, M. Adams, J. Good, P. Kelton, E. Barker, P. Palunas, F. Bash, L. Ramsey, G. Hill, P. MacQueen, M. Cornell, E. Robinson, “The Hobby-Eberly Telescope Completion Project,” SPIE **4837**-109, Waikoloa, HI, August 2002.
3. M. Adams, P. Palunas, J. Booth, J. Fowler, M. Wolf, G. Ames, E. Montgomery, J. Rakoczy, “Hobby-Eberly Telescope segment alignment maintenance system,” SPIE **4837**-80, Waikoloa, HI, August 2002.
4. J. Rakoczy, D. Hall, R. Howard, W. Ly, J. Weir, E. Montgomery, M. Adams, J. Booth, J. Fowler, G. Ames, “Primary Mirror Figure Maintenance of the Hobby-Eberly Telescope using the Segment Alignment Maintenance System,” SPIE **4837**-81, Waikoloa, HI, August 2002.
5. J. Good, P. Kelton, J. Booth, E. Barker, "The Hobby-Eberly Telescope Natural Ventilation System Upgrade," SPIE **4837**-26, Waikoloa, HI, August 2002.
6. M. Wolf, M. Ward, J. Booth, B. Roman, “Polarization shearing laser interferometer for aligning segmented telescope mirrors,” SPIE **4837**-88, Waikoloa, HI, August 2002.
7. E. Barker, M. Adams, F. Delgman, V. Riley, T. George, J. Booth, A. Rest, E. Robinson, “Determination of the Intrinsic Site Seeing for the Hobby-Eberly Telescope,” SPIE **4837**-25, Waikoloa, HI, August 2002.
8. D. Pileri, V. Krabbendam, “Hobby-Eberly primary mirror fabrication,” SPIE **2536**, 344-349, San Diego, CA, July 1995.
9. D. O’Donoghue, A. Swat, “Global Radius of Curvature Control for SALT,” 6 August 2001.
10. A. Swat, “Image Quality vs Global Radius of Curvature,” SALT Technical Report: Document 1000AA040.